THE JOURNAL OF PHYSICAL CHEMISTRY Letters

Letter

pubs.acs.org/JPCL

# Interface for Light-Driven Electron Transfer by Photosynthetic Complexes Across Block Copolymer Membranes

Liangju Kuang,[†,§] Tien L. Olson,[‡,§] Su Lin,[‡] Marco Flores,[‡] Yunjiang Jiang,[†] Wan Zheng,[†] JoAnn C. Williams,[‡] James P. Allen,*[,‡] and Hongjun Liang*[,†]

[†]Department of Metallurgical and Materials Engineering, Colorado School of Mines, Golden, Colorado 80401, United States

[‡]Department of Chemistry and Biochemistry, Arizona State University, Tempe, Arizona 85287, United States

Supporting Information

**ABSTRACT:** Incorporation of membrane proteins into nanodevices to mediate recognition and transport in a collective and scalable fashion remains a challenging problem. We demonstrate how nanoscale photovoltaics could be designed using robust synthetic nanomembranes with incorporated photosynthetic reaction centers (RCs). Specifically, RCs from *Rhodobacter sphaeroides* are reconstituted spontaneously into rationally designed polybutadiene membranes to form hierarchically organized proteopolymer membrane arrays via a charge-interaction-directed reconstitution mechanism. Once incorporated, the RCs are fully active for prolonged periods based upon a variety of spectroscopic measurements, underscoring preservation of their 3D pigment configuration critical for light-driven charge transfer. This result provides a strategy to construct solar conversion devices using structurally versatile proteopolymer membranes with integrated RC functions to harvest broad regions of the solar spectrum.

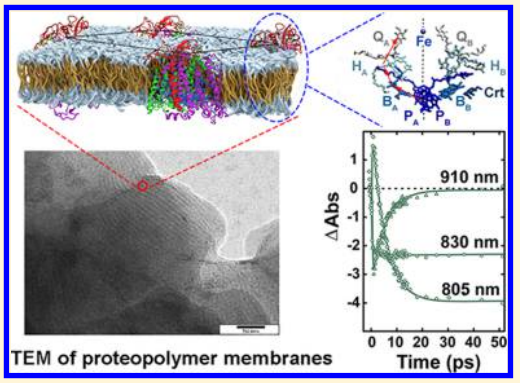


**SECTION:** Biophysical Chemistry and Biomolecules

A key challenge in renewable energy is to capture, convert, and store solar power with earth-abundant materials and environmentally benign technologies.[1−3] Photosynthesis realizes light energy conversion on a grand scale using membrane proteins (MPs), such as reaction centers (RCs), which evolutionarily couple their absorption spectra to solar flux[4] to mediate light-driven charge separation across an embedding lipid bilayer through a three-dimensional (3D) configuration of pigment cofactors precisely held by a protein framework.[5,6] The use of chlorophyll cofactors derived from photosynthetic complexes as renewable sensitizers for solar conversion has attracted much attention.[4,7−10] However, hierarchical assembly of different dye molecules in a 3D configuration at the nanoscale to mimic the highly efficient light-harvesting and electron-transfer functions inherent to photosystems has not been achieved.[9−11] Ideally, photosynthetic complexes could be used as biologically derived high-performance energy materials. RCs can be expressed in sizable quantities and stably purified from their cellular environment as detergent-solubilized forms. Incorporation of RCs into solar energy conversion devices, such as dye-sensitized solar cells (DSSCs),[12] would improve the photoresponse in the red and near-infrared regions and reduce reliance on resource-limited dyes.[7,12] Photoelectric functions of detergent-solubilized photosynthetic complexes tethered on various substrates have been examined,[13−18] but harnessing their light-activated charge separation collectively in a scalable fashion is contingent on the inclusion of these MPs into a supporting nanomembrane. RCs have been incorporated into lipid bilayers for many years,[19−21] but the fluidic and labile nature of lipid bilayers has limited their use in engineered systems. To overcome these limitations, we have designed synthetic block copolymers that induce spontaneous reconstitution of RCs to form hierarchically organized proteopolymer membrane arrays, which are layered proteopolymer membranes coupled with 2D rectangular lattices of RCs embedded in individual membrane layers (Figure 1). The RCs were shown to be fully active in the nanomembranes using steady-state and time-resolved spectroscopic probing methods.

The RC from *Rhodobacter (Rb.) sphaeroides* has three protein subunits (shown in green, purple, and red in Figure 1, left panel), which hold 10 cofactors in two quasi-symmetrical branches (A, B) related to each other via a C2 axis (Figure 1, right panel).[6] The axis runs through an excitonically coupled bacteriochlorophyll (BChl) dimer ($P_A$, $P_B$) that serves as an electron-hole-pair generator and an iron atom across the protein. The other two BChls ($B_A$, $B_B$), bacteriopheophytins (BPheos; $H_A$, $H_B$) and quinones ($Q_A$, $Q_B$), spread along the two branches symmetrically. A single carotenoid (Crt) cofactor, associated with the B branch, provides photoprotection.[22] Light-induced electron transfer occurs along the A branch from P to $Q_A$ (red arrows in Figure 1) in ∼200 ps with 100%

**Received:** December 23, 2013
**Accepted:** February 5, 2014
**Published:** February 5, 2014



  

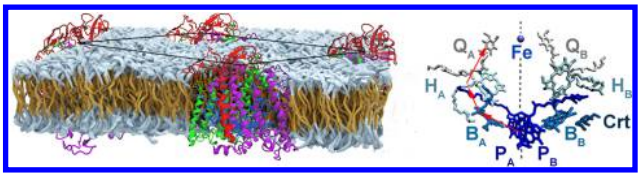


**Figure 1.** Schematic representations show a 2D rectangular proteopolymer lattice (left) with spontaneously reconstituted RCs from *Rb. sphaeroides* and a 3D arrangement of the 10 cofactors precisely held by individual RCs embedded across the membrane (right). The RC-supporting polymer membranes consist of amphiphilic triblock copolymers (represented as curved strings with hydrophobic middle blocks in yellow and hydrophilic end blocks in white). The L, M, and H subunits of RCs are represented in green, purple, and red, respectively. The 10 cofactors within individual RCs are represented in stick models with different colors.

quantum efficiency and produces a stable (lifetime ~0.1 s) electron-hole-pair (i.e., $P^{\bullet+}Q_A^{\bullet-}$) across the RC-supporting membrane with a large open-circuit voltage (~0.7 V). This highly efficient photovoltaic function has great potential in engineered systems that could make use of the spontaneous and functional reconstitution of RCs into synthetic membranes, as described below.

Previously, we developed a charge-interaction-directed reconstitution (CIDR) method[23,24] to induce spontaneous and functional reconstitution of proteorhodopsin, a light-driven proton pump consisting of seven transmembrane helices and one cofactor,[25] into amphiphilic block copolymer membranes with different membrane moduli.[26,27] These findings differ from other proteopolymer studies that focused on fluidic polymer membranes in a viscous-flow state[28−31] and suggest a different mechanism of reconstitution: while conventional MP reconstitution approaches rely critically on detergent or mechanical means to destabilize membranes followed by a delicate detergent removal process,[28−32] CIDR occurs spontaneously and needs no external help.[23,24,26,27]

We synthesized two well-defined amphiphilic triblock copolymers, $PBD_{22}$-*b*-$(P4MVP_{28})_2$ and $PBD_{56}$-*b*-$(P4MVP_{29})_2$, which self-assemble in water into liposome-mimicking polymersomes (see the Supporting Information, SI). Increasing the membrane-forming block from $PBD_{22}$ to $PBD_{56}$ enlarges the membrane thickness from 31 to 49 Å and drives a transition of the PBD chain motion mode from Rouse dynamics to entanglement release,[26] which further strengthens the membrane. Because the isoelectric point of RCs solubilized using lauryl dimethylamine oxide (LDAO) is 6.1,[33] CIDR was performed at pH = 8, where the two extramembrane regions of RCs are anionically and asymmetrically charged. The oppositely charged polymersome membranes induce spontaneous reconstitution of RCs into condensed proteopolymer complexes without using any external means for detergent removal. The condensed proteopolymer complexes are separated from the rest of the supernatant for structural characterizations and functional assays. Using a transmission electron microscope (TEM), a striking morphological transition from spherical polymersomes to a multilamellar structure with a periodicity of ~75 Å is revealed in both complexes (Figure 2b,c). This spacing does not physically fit any forms of random flocculation between polymersome membranes and LDAO-solubilized RCs. The spacing is attributed to stacked proteopolymer membrane arrays of reconstituted RCs as RCs have a transmembrane dimension of 70 Å[34] and polymersome membranes are known to accommodate the dimension of reconstituted MPs via

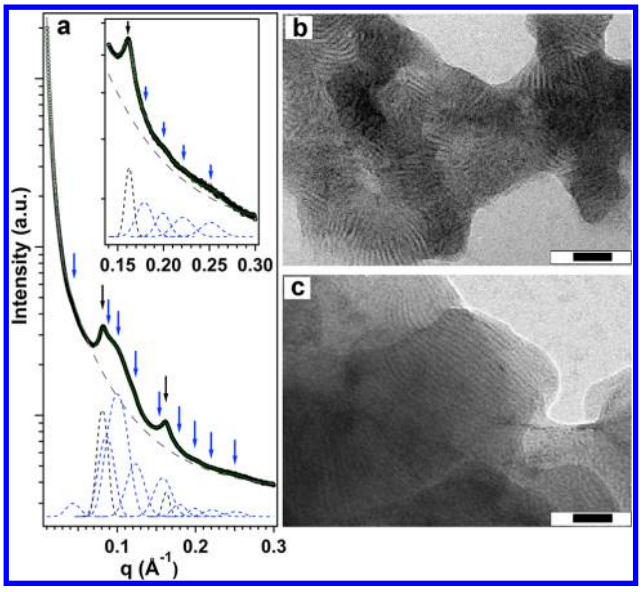


**Figure 2.** CIDR of RCs from *Rb. sphaeroides* in PBD-based polymersome membranes. (a) Synchrotron SAXS of proteopolymer complexes comprised of RCs and $PBD_{22}$-*b*-$(P4MVP_{28})_2$. The scattering data (○) are fitted to resolve a background (gray dashed line) and two sets of structural features: a multilamellar proteopolymer membrane (black dotted peaks, $q_{001}$ = 0.081 Å$^{-1}$) and a 2D rectangular RC lattice within individual membranes (blue dotted peaks centered at 0.044, 0.086, 0.099, 0.123, 0.158, 0.179, 0.199, 0.22, and 0.25 Å$^{-1}$, corresponding to $q_{10}$, $q_{01}$, $q_{11}$, $q_{21}$, $q_{31}$, $q_{12}$, $q_{22}$ (or $q_{41}$), $q_{32}$, and $q_{42}$, respectively). (Inset) A blow-out of the $q$ = 0.14−0.3 Å$^{-1}$ range. Summation of fitted contributions (green solid line) overlaps nicely with the scattering data. TEM confirms similar multilamellar proteopolymer complexes comprised of (b) RCs and $PBD_{22}$-*b*-$(P4MVP_{28})_2$ and (c) RCs and $PBD_{56}$-*b*-$(P4MVP_{29})_2$ (scale bar: 50 nm).

hydrophobic matching.[35] The success of CIDR was further confirmed by synchrotron small-angle X-ray scattering (SAXS) studies (Figure 2a): besides two harmonics (black arrows) revealing a multilamellar structure spaced 78 Å apart ($q_{001}$ = 0.081 Å$^{-1}$) that agrees well with TEM, in-membrane RC correlations are clearly discernible (blue arrows). These peaks are fitted best with a rectangular lattice of $a$ = 142 Å and $b$ = 72 Å (shown schematically in Figure 1). Note that a set of its first nine peaks (up to $q_{42}$, inset) is clearly resolved with a consistent full width at half-maximum (FWHM, ~0.020−0.025 Å$^{-1}$) and form factor, although $q_{10}$ is shadowed by strong scattering in the vicinity of the beam stop and appears weak. To the best of our knowledge, this is the first observation that RCs can be spontaneously reconstituted into a 2D lattice in block copolymer membranes. This 2D proteopolymer lattice is surprisingly similar to the basal plane of various forms of RC 3D crystals,[36] suggesting a consistent packing arrangement defined by the protein itself.

We examined whether the polymersome membranes, which are much more robust than lipid bilayers[37] yet still flexible due to the low glass transition temperature of PBD ($T_g^{PBD} \approx 218$ K),[38] would incorporate RCs that retain their structural and functional states. The spectral characteristics of RCs depend critically on the 3D configuration of cofactors and hence can be used as sensitive indicators of any change in the pigment organization or interactions with the protein environment. The three distinct maxima at 865, 804, and 760 nm in the steady-state absorption spectra arise from the BChl dimer P, BChl


dx.doi.org/10.1021/jz402766y | J. Phys. Chem. Lett. 2014, 5, 787−791

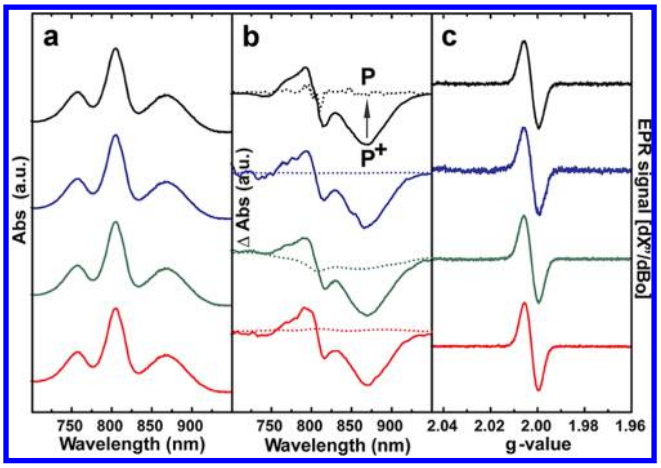


**Figure 3.** Characteristic spectra of RCs are similar when solubilized by LDAO (black) and embedded in WT-NA chromatophores (blue), $PBD_{22}$ membranes (green), and $PBD_{56}$ membranes (red). (a) Steady-state absorption spectra. (b) Light-minus-dark difference optical absorption spectra (solid line: illuminated; dashed line: 3 min after light removed). (c) Light-induced EPR spectra. All spectra have been normalized.

monomers, and BPheos, respectively (Figure 3a). These features are identical for wild-type (WT) RCs solubilized using LDAO (black trace), WT-NA chromatophores (blue), that is, antenna-less RC-containing membrane fragments, as well as RCs reconstituted in $PBD_{22}$ (green) and $PBD_{56}$ membranes (red). This suggests that the pigment−pigment and pigment−RC interactions are not disrupted when RCs are reconstituted into block copolymer membranes and that the polymer membranes provide an excellent amphiphilic environment to stabilize the RC complexes.

The light-minus-dark difference optical absorption spectra of RCs were also compared (Figure 3b). Terbutryn was added to block electron transfer from $Q_A$ to $Q_B$; therefore, only the $P^{\bullet+}Q_A^{\bullet-}$ state was formed upon illumination. For each of the samples, we observed the same $P^{\bullet+}Q_A^{\bullet-}$ formation (solid line); generation of the $P^{\bullet+}$ species causes a loss of absorbance at 865 nm, and the presence of $Q_A^{\bullet-}$ results in electrochromic shifts of the BChls and BPheos. We confirmed the complete reversibility of this charge separation ($P^{\bullet+}Q_A^{\bullet-} \rightarrow PQ_A$) in all cases after light was removed (dashed line). The proteopolymer membranes were fully active for several weeks during their storage in the dark.

Electron paramagnetic resonance (EPR) spectroscopy is a sensitive measure of the oxidized state of the primary electron donor $P^{\bullet+}$. The magnetic field was calibrated using isolated WT RCs as a $g$ value standard at 2.0026.[39] The continuous wave (CW) EPR spectra in all preparations show a narrow signal (10 G) with the same $g$ value, within the error (±0.0003), as WT RCs (Figure 3c); this demonstrates an unaltered electronic structural arrangement of P in the proteopolymer membranes.

To examine whether the RC-mediated electron-transfer pathway is membrane-dependent, we applied ultrafast transient absorption spectroscopy to characterize the RCs in WT-NA chromatophores and PBD membranes (Figure 4). The spectra measured 0.5 ps after illumination (dashed lines) represent a typical spectral profile of the excited state P*, dominated by a bleaching at 870 nm that extends to the 920 nm region.[40] The initial electron transfer from P* forming $P^{\bullet+}H_A^{\bullet-}$ has been shown to be multiexponential in the WT RCs,[40,41] with time

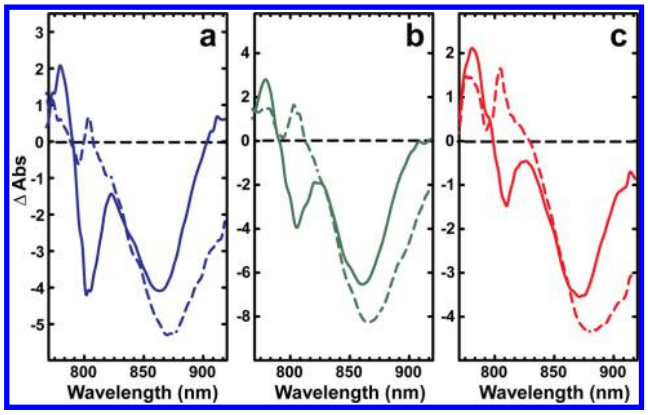


**Figure 4.** Transient absorption light-minus-dark spectra of RCs in (a) WT-NA chromatophores and (b) $PBD_{22}$ and (c) $PBD_{56}$ membranes recorded at 0.5 (dashed lines) and 100 ps (solid lines) after illumination with a saturating laser pulse.

constants of 2.8−3.5 and 10−12 ps, or a single exponential lifetime of 3−5 ps. Because sodium dithionite was added to prereduce $Q_A$, the final state is $P^{\bullet+}H_A^{\bullet-}$, which lives for 10−20 ns,[40] and the spectra measured at 100 ps (solid lines) consist of features well-documented for that state,[42] as confirmed by an analysis using evolution-associated difference spectra (Figure S2, SI). We could not detect the small population of transient state $P^{\bullet+}B_A^{\bullet-}$ because the $P^{\bullet+}B_A^{\bullet-} \rightarrow P^{\bullet+}H_A^{\bullet-}$ reaction is faster than that for $P^* \rightarrow P^{\bullet+}B_A^{\bullet-}$ (1 versus 3 ps).[43] For the $PBD_{56}$ membranes, the absorption change at 910 nm does not recover to zero, resulting in an increased contribution from $P^{\bullet+}$ at that wavelength; the signal does recover to zero at wavelengths longer than 917 nm. These essentially identical spectra of RCs embedded in native and different synthetic membranes suggest that the RC-mediated electron-transfer properties are insensitive to variations of supporting membranes.

We examined whether the light-driven, cross-membrane charge separation is regulated by RC-supporting membranes using time-resolved spectroscopy to track the electron-transfer kinetics when P and the BChl monomers were excited with 600 nm light (Figure 5). The kinetic traces at 910 nm represent

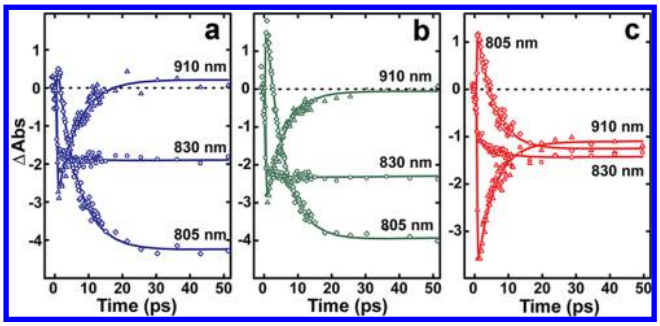


**Figure 5.** Kinetics traces of RCs in (a) WT-NA chromatophores and (b) $PBD_{22}$ and (c) $PBD_{56}$ membranes recorded at 910 (triangles), 805 (diamonds), and 830 nm (circles). Lines are theoretical fits by ASUFIT (see the SI for details).

mainly the decay of P*. As energy transfer from the BChl monomers to P takes ∼100 fs,[40] the P* population was fully developed within 200 fs, as seen by a rapid loss of absorbance in the 910 nm kinetic trace. The recovery of the bleaching signal at 910 nm is accompanied by a bleaching increase at 805 nm due to the $B_A$ ground-state absorbance shift, resulting from


dx.doi.org/10.1021/jz402766y | J. Phys. Chem. Lett. 2014, 5, 787−791

formation of $P^{\bullet+}H_A^{\bullet-}$ from P* via $P^{\bullet+}B_A^{\bullet-}$.[43] The P* stimulated emission decay, as well as the kinetics at 805 nm, is very similar in all samples. The kinetics at 830 nm show that there was no P recovery or no change in the $P^{\bullet+}H_A^{\bullet-}$ population up to hundreds of ps, indicating that there is no yield loss during electron transfer for RCs embedded in both native and synthetic nanomembranes.

In summary, we demonstrate that spontaneous reconstitution of the RCs from *Rb. sphaeroides*, a photosynthetic complex comprised of 3 protein subunits and 10 cofactors, into block copolymer nanomembranes of different moduli is achieved via the CIDR mechanism. We show unambiguously that the structural and functional integrity of the RCs is maintained in the proteopolymer membranes. While MP-supporting lipid bilayers are recognized as allosteric regulators for MP functions,[44−46] the RCs are fully functional in the synthetic membranes, underscoring preservation of their 3D pigment configuration critical for light-driven charge transfer and suggesting that other MPs can be incorporated similarly into robust synthetic membranes in a fully functional form. Compared to previous studies on segregated, disordered photosynthetic complexes deposited on various substrates, spontaneous reconstitution of light conversion RCs into ordered proteopolymer nanomembranes is a significant step forward. It enables directed assembly of scalable photovoltaic nanomembranes on various engineered devices using oriented RCs tethered on electrodes as templates, as has been shown previously for reconstitution of supported cytochrome *c* oxidase in lipid bilayers.[47] This approach allows the use of robust and structurally versatile block copolymers in place of lipid bilayers to stabilize and interface RCs with a supporting substrate in desirable proteomembrane configurations for efficient electron transfer,[13−18] and provides the opportunity to create photoelectrical or photochemical devices that harness RC functions collectively for conversion of solar energy through an enhanced spectral region.

## ■ ASSOCIATED CONTENT

### Supporting Information

Experimental details on the synthesis and characterization of block copolymers and polymersomes, expression and purification of RCs, CIDR of proteopolymer complexes and their structural characterization, EPR and optical spectroscopies, and EADS. This material is available free of charge via the Internet at http://pubs.acs.org.

## ■ AUTHOR INFORMATION


### Corresponding Authors

*E-mail: jallen@asu.edu (J.P.A.).
*E-mail: hjliang@mines.edu (H.L.).

### Author Contributions

[§]L.K. and T.L.O. contributed equally.


### Notes

The authors declare no competing financial interest.

## ■ ACKNOWLEDGMENTS

This work was supported partially by a seed grant from REMRSEC (DMR-0820518) and the Grant CBET-1160291 (to H.L.), as well as by the Grant CHE 1158552 (to J.P.A. and J.C.W.) from the National Science Foundation. SAXS experiments were performed at the Stanford Synchrotron Radiation Lightsource, a Directorate of SLAC National Accelerator Laboratory and an Office of Science User Facility operated for the U.S. Department of Energy Office of Science by Stanford University.

## ■ REFERENCES


(1) Lewis, N. S.; Nocera, D. G. Powering the Planet: Chemical Challenges in Solar Energy Utilization. *Proc. Natl. Acad. Sci. U.S.A.* **2006**, *103*, 15729−15735.

(2) Gust, D.; Moore, T. A.; Moore, A. L. Mimicking Photosynthetic Solar Energy Transduction. *Acc. Chem. Res.* **2001**, *34*, 40−48.

(3) Blankenship, R. E.; Tiede, D. M.; Barber, J.; Brudvig, G. W.; Fleming, G.; Ghirardi, M.; Gunner, M. R.; Junge, W.; Kramer, D. M.; Melis, A.; et al. Comparing Photosynthetic and Photovoltaic Efficiencies and Recognizing the Potential for Improvement. *Science* **2011**, *332*, 805−809.

(4) Kruse, O.; Rupprecht, J.; Mussgnug, J. H.; Dismukes, G. C.; Hankamer, B. Photosynthesis: A Blueprint for Solar Energy Capture and Biohydrogen Production Technologies. *Photochem. Photobiol. Sci.* **2005**, *4*, 957−970.

(5) Moser, C. C.; Keske, J. M.; Warncke, K.; Farid, R. S.; Dutton, P. L. Nature of Biological Electron Transfer. *Nature* **1992**, *355*, 796−802.

(6) Allen, J. P.; Feher, G.; Yeates, T. O.; Komiya, H.; Rees, D. C. Structure of the Reaction Center from *Rhodobacter sphaeroides* R-26: The Cofactors. *Proc. Natl. Acad. Sci. U.S.A.* **1987**, *84*, 5730−5734.

(7) McHale, J. L. Hierarchal Light-Harvesting Aggregates and Their Potential for Solar Energy Applications. *J. Phys. Chem. Lett.* **2012**, *3*, 587−597.

(8) Gust, D.; Moore, T. A.; Moore, A. L. Realizing Artificial Photosynthesis. *Faraday Discuss.* **2012**, *155*, 9−26.

(9) Balaban, T. S. Tailoring Porphyrins and Chlorins for Self-Assembly in Biomimetic Artificial Antenna Systems. *Acc. Chem. Res.* **2005**, *38*, 612−623.

(10) Modesto-Lopez, L. B.; Thimsen, E. J.; Collins, A. M.; Blankenship, R. E.; Biswas, P. Electrospray-Assisted Characterization and Deposition of Chlorosomes to Fabricate a Biomimetic Light-Harvesting Device. *Energy Environ. Sci.* **2010**, *3*, 216−222.

(11) Benniston, A. C.; Harriman, A. Artificial Photosynthesis. *Mater. Today* **2008**, *11*, 26−34.

(12) Gratzel, M. Recent Advances in Sensitized Mesoscopic Solar Cells. *Acc. Chem. Res.* **2009**, *42*, 1788−1798.

(13) Das, R.; Kiley, P. J.; Segal, M.; Norville, J.; Yu, A. A.; Wang, L. Y.; Trammell, S. A.; Reddick, L. E.; Kumar, R.; Stellacci, F.; et al. Integration of Photosynthetic Protein Molecular Complexes in Solid-State Electronic Devices. *Nano Lett.* **2004**, *4*, 1079−1083.

(14) Esper, B.; Badura, A.; Rogner, M. Photosynthesis as a Power Supply for (Bio-)Hydrogen Production. *Trends Plant Sci.* **2006**, *11*, 543−549.

(15) Carmeli, I.; Mangold, M.; Frolov, L.; Zebli, B.; Carmeli, C.; Richter, S.; Holleitner, A. W. A Photosynthetic Reaction Center Covalently Bound to Carbon Nanotubes. *Adv. Mater.* **2007**, *19*, 3901−3905.

(16) Grimme, R. A.; Lubner, C. E.; Bryant, D. A.; Golbeck, J. H. Photosystem I/Molecular Wire/Metal Nanoparticle Bioconjugates for the Photocatalytic Production of $H_2$. *J. Am. Chem. Soc.* **2008**, *130*, 6308−6309.

(17) Kim, I.; Bender, S. L.; Hranisavljevic, J.; Utschig, L. M.; Huang, L. B.; Wiederrecht, G. P.; Tiede, D. M. Metal Nanoparticle Plasmon-Enhanced Light-Harvesting in a Photosystem I Thin Film. *Nano Lett.* **2011**, *11*, 3091−3098.

(18) Lebedev, N.; Trammell, S. A.; Spano, A.; Lukashev, E.; Griva, I.; Schnur, J. Conductive Wiring of Immobilized Photosynthetic Reaction Center to Electrode by Cytochrome *c*. *J. Am. Chem. Soc.* **2006**, *128*, 12044−12045.

(19) Gopher, A.; Blatt, Y.; Schonfeld, M.; Okamura, M. Y.; Feher, G.; Montal, M. The Effect of an Applied Electric-Field on the Charge Recombination Kinetics in Reaction Centers Reconstituted in Planar Lipid Bilayers. *Biophys. J.* **1985**, *48*, 311−320.

(20) Alegria, G.; Dutton, P. L. Langmuir−Blodgett Monolayer Films of Bacterial Photosynthetic Membranes and Isolated Reaction Centers: Preparation, Spectrophotometric and Electrochemical Characterization. *Biochim. Biophys. Acta* **1991**, *1057*, 239−257.
(21) Kobayashi, M.; Fujioka, Y.; Mori, T.; Terashima, M.; Suzuki, H.; Shimada, Y.; Saito, T.; Wang, Z. Y.; Nozawa, T. Reconstitution of Photosynthetic Reaction Centers and Core Antenna-Reaction Center Complexes in Liposomes and Their Thermal Stability. *Biosci., Biotechnol., Biochem.* **2005**, *69*, 1130−1136.
(22) Slouf, V.; Chabera, P.; Olsen, J. D.; Martin, E. C.; Qian, P.; Hunter, C. N.; Polivka, T. Photoprotection in a Purple Phototrophic Bacterium Mediated by Oxygen-Dependent Alteration of Carotenoid Excited-State Properties. *Proc. Natl. Acad. Sci. U.S.A.* **2012**, *109*, 8570−8575.
(23) Liang, H. J.; Whited, G.; Nguyen, C.; Stucky, G. D. The Directed Cooperative Assembly of Proteorhodopsin into 2D and 3D Polarized Arrays. *Proc. Natl. Acad. Sci. U.S.A.* **2007**, *104*, 8212−8217.
(24) Liang, H. J.; Whited, G.; Nguyen, C.; Okerlund, A.; Stucky, G. D. Inherently Tunable Electrostatic Assembly of Membrane Proteins. *Nano Lett.* **2008**, *8*, 333−339.
(25) Beja, O.; Aravind, L.; Koonin, E. V.; Suzuki, M. T.; Hadd, A.; Nguyen, L. P.; Jovanovich, S. B.; Gates, C. M.; Feldman, R. A.; Spudich, J. L.; et al. Bacterial Rhodopsin: Evidence for a New Type of Phototrophy in the Sea. *Science* **2000**, *289*, 1902−1906.
(26) Hua, D. B.; Kuang, L. J.; Liang, H. J. Self-Directed Reconstitution of Proteorhodopsin with Amphiphilic Block Copolymers Induces the Formation of Hierarchically Ordered Proteopolymer Membrane Arrays. *J. Am. Chem. Soc.* **2011**, *133*, 2354−2357.
(27) Kuang, L. J.; Fernandes, D. A.; O'Halloran, M.; Zheng, W.; Jiang, Y. J.; Ladizhansky, V.; Brown, L. S.; Liang, H. J. "Frozen" Block Copolymer Nanomembranes with Light-Driven Proton Pumping Performance. *ACS Nano* **2014**, *8*, 537−545.
(28) Meier, W.; Nardin, C.; Winterhalter, M. Reconstitution of Channel Proteins in (Polymerized) ABA Triblock Copolymer Membranes. *Angew. Chem., Int. Ed.* **2000**, *39*, 4599−4602.
(29) Choi, H. J.; Montemagno, C. D. Artificial Organelle: ATP Synthesis from Cellular Mimetic Polymersomes. *Nano Lett.* **2005**, *5*, 2538−2542.
(30) Ihle, S.; Onaca, O.; Rigler, P.; Hauer, B.; Rodriguez-Ropero, F.; Fioroni, M.; Schwaneberg, U. Nanocompartments with a pH Release System Based on an Engineered OmpF Channel Protein. *Soft Matter* **2011**, *7*, 532−539.
(31) Zhang, X. Y.; Tanner, P.; Graff, A.; Palivan, C. G.; Meier, W. Mimicking the Cell Membrane with Block Copolymer Membranes. *J. Polym. Sci., Part A: Polym. Chem.* **2012**, *50*, 2293−2318.
(32) Rigaud, J. L.; Levy, D. Reconstitution of Membrane Proteins into Liposomes. *Methods Enzymol.* **2003**, *372*, 65−86.
(33) Prince, R. C.; Cogdell, R. J.; Crofts, A. R. The Photo-Oxidation of Horse Heart Cytochrome *c* and Native Cytochrome $c_2$ by Reaction Centres from *Rhodopseudomonas spheroides* R26. *Biochim. Biophys. Acta, Bioenerg.* **1974**, *347*, 1−13.
(34) Allen, J. P.; Feher, G.; Yeates, T. O.; Komiya, H.; Rees, D. C. Structure of the Reaction Center from *Rhodobacter sphaeroides* R-26: The Protein Subunits. *Proc. Natl. Acad. Sci. U.S.A.* **1987**, *84*, 6162−6166.
(35) Pata, V.; Dan, N. The Effect of Chain Length on Protein Solubilization in Polymer-Based Vesicles (Polymersomes). *Biophys. J.* **2003**, *85*, 2111−2118.
(36) Allen, J. P. Crystallization of the Reaction Center from *Rhodobacter sphaeroides* in a New Tetragonal Form. *Proteins: Struct., Funct., Genet.* **1994**, *20*, 283−286.
(37) Discher, D. E.; Eisenberg, A. Polymer Vesicles. *Science* **2002**, *297*, 967−973.
(38) Brandrup, J.; Immergut, E. H.; Grulke, E. A.; Abe, A.; Bloch, D. R. *Polymer Handbook*, 4th ed.; John Wiley & Sons: New York, 2005.
(39) McElroy, J. D.; Feher, G.; Mauzerall, D. C. On the Nature of the Free Radical Formed During the Primary Process of Bacterial Photosynthesis. *Biochim. Biophys. Acta* **1969**, *172*, 180−183.
(40) Woodbury, N. W. T.; Allen, J. P. The Pathway and Thermodynamics of Electron Transfer in Wild Type and Mutant Reaction Centers of Purple Non-Sulfur Bacteria. In *Anoxygenic Photosynthetic Bacteria*; Blankenship, R. E., Madigan, M. T., Bauer, C. E., Eds.; Kluwer Academic Publishers: New York, 1995; pp 527−557.
(41) Wang, H. Y.; Lin, S.; Allen, J. P.; Williams, J. C.; Blankert, S.; Laser, C.; Woodbury, N. W. Protein Dynamics Control the Kinetics of Initial Electron Transfer in Photosynthesis. *Science* **2007**, *316*, 747−750.
(42) Ogrodnik, A.; Keupp, W.; Volk, M.; Aumeier, G.; Michel-Beyerle, M. E. Inhomogeneity of Radical Pair Energies in Photosynthetic Reaction Centers Revealed by Differences in Recombination Dynamics of $P^+H_A^-$ When Detected in Delayed Emission and in Absorption. *J. Phys. Chem.* **1994**, *98*, 3432−3439.
(43) Carter, B.; Boxer, S. G.; Holten, D.; Kirmaier, C. Photochemistry of a Bacterial Photosynthetic Reaction Center Missing the Initial Bacteriochlorophyll Electron Acceptor. *J. Phys. Chem. B* **2012**, *116*, 9971−9982.
(44) Phillips, R.; Ursell, T.; Wiggins, P.; Sens, P. Emerging Roles for Lipids in Shaping Membrane−Protein Function. *Nature* **2009**, *459*, 379−385.
(45) Andersen, O. S.; Koeppe, R. E. Bilayer Thickness and Membrane Protein Function: An Energetic Perspective. *Annu. Rev. Biophys. Biomol. Struct.* **2007**, *36*, 107−130.
(46) Brown, M. F. Curvature Forces in Membrane Lipid−Protein Interactions. *Biochemistry* **2012**, *51*, 9782−9795.
(47) Ataka, K.; Giess, F.; Knoll, W.; Naumann, R.; Haber-Pohlmeier, S.; Richter, B.; Heberle, J. Oriented Attachment and Membrane Reconstitution of His-Tagged Cytochrome *c* Oxidase to a Gold Electrode: *In Situ* Monitoring by Surface-Enhanced Infrared Absorption Spectroscopy. *J. Am. Chem. Soc.* **2004**, *126*, 16199−16206.